

Ising Model with First-, Second-, and Third-Neighbor Interactions

Joel Philhours

Department of Physics and Astronomy, University of Kentucky, Lexington, Kentucky 40506

(Received 16 February 1971)

The high-temperature expansion of the partition function of an Ising model in zero magnetic field is calculated through terms of T^{-9} for a fcc lattice and variable first-, second-, and third-neighbor interactions (J_1 , J_2 , and J_3). Values of the transition temperature T_c and of the first-, second-, and third-neighbor correlation coefficients at $T=T_c$ are given for J_2/J_1 and J_3/J_1 each varying between 0 and 2.

I. INTRODUCTION

The usual method¹ of performing a high-temperature expansion of the Ising model makes use of the relation

$$e^{gJ/kT} = \cosh(J/kT)[1 + g \tanh(J/kT)] \quad (g = \pm 1) \quad (1)$$

to obtain a series in powers of $\tanh(J/kT)$. We have chosen to write the exponential series of the Boltzmann factor and thereby get directly a power series in J/kT . The high-temperature expansion of the partition function is given through $(1/kT)^9$ for a fcc lattice with variable first-, second-, and third-neighbor interactions. Values of the transition temperature and of the first-, second-, and third-neighbor correlation coefficients are calculated under the assumption that the specific heat has the form²

$$C \sim (1 - T_c/T)^{-1/8}, \quad T \rightarrow T_c^+ \quad (2)$$

above the transition temperature T_c .

In Sec. II we outline how the contributions may be considered as a product of two terms—one being independent of the lattice and interactions and the other being a lattice sum depending on the lattice and interactions. This has been known^{1,3} for some time, but it is presented here since we have a slightly different approach and interpretation.

The values of the transition temperature and the correlation coefficients are presented in Sec. III. The same calculations are performed for a "generalized" spherical model^{4,5} and the results are compared with those of the Ising model in Sec. IV.

II. EXPANSION OF $\ln Z$

We wish to obtain a high-temperature expansion of the partition function. Once this expansion has been obtained, various properties may be determined, e.g., the energy, the specific heat, the correlation coefficients for distances at which there are interactions, and the transition temperature (assuming that the high-temperature series have assumed their asymptotic form for these early coefficients). The approach is similar to that of several other authors³ with the special case

of zero magnetic field being considered in this paper. However, the grouping of terms and their characterization is slightly different in this paper and a full description will be presented.

The partition function is given by

$$Z^N = \frac{1}{2^N} \sum_{\sigma_{\mathbf{i},\mathbf{j}}} \exp \left(\frac{1}{2} \beta \sum_{\mathbf{i},\mathbf{j}} J_{\mathbf{i},\mathbf{j}} \sigma_{\mathbf{i}} \sigma_{\mathbf{j}} \right), \quad (3)$$

where Z is the partition function per site in a collection of N sites, the factor $1/2^N$ has been inserted to yield $Z=1$ for no interactions, $\beta=1/kT$, the sum $\sum_{\sigma_{\mathbf{i},\mathbf{j}}}$ means N sums, the i th one of which is $\sum_{\sigma_{\mathbf{i},\mathbf{j}}}$, and $\sum_{\mathbf{i},\mathbf{j}}$ means \mathbf{i} and \mathbf{j} are summed over the lattice vectors independently of each other. The high-temperature expansion is obtained by writing

$$Z^N = \frac{1}{2^N} \sum_{n=0}^{\infty} \left[\frac{\beta^n}{n!} \sum_{\sigma_{\mathbf{i},\mathbf{j}}} \left(\frac{1}{2} \sum_{\mathbf{i},\mathbf{j}} J_{\mathbf{i},\mathbf{j}} \sigma_{\mathbf{i}} \sigma_{\mathbf{j}} \right)^n \right]. \quad (4)$$

The performance of the sum $\sum_{\sigma_{\mathbf{i},\mathbf{j}}}$ yields contributions only when each $\sigma_{\mathbf{i}}$ occurs an even number of times and in the end cancels the $1/2^N$ factor in the above equation. For a given value of n , a power series in N will result. However, the quantity that is needed is $\ln Z$, and it is easily shown that $\ln Z$ is obtained by taking the coefficient of N in Z^N , i.e.,

$$\ln Z = \sum_{n=2}^{\infty} R_n \beta^n, \quad (5)$$

where R_n is the coefficient of $N\beta^n$ in Z^N .

It is well known^{1,3} that the contributions may be analyzed in terms of constructing graphs on the lattice. With the factor $J_{\mathbf{i},\mathbf{j}}$ we associate a bond connecting sites \mathbf{i} and \mathbf{j} on the lattice. A contributing term to R_n may then be represented by a graph in which the number of bonds is equal to n and each vertex in the graph is joined by an even number of bonds.

The graph itself may be described by means of δ -function restrictions on the vectors that form the graph. We will group contributions according to their δ -function description (DFD). The contribution of a particular DFD may be considered as the product of two factors: a coefficient and a lattice

sum. The coefficient results mainly from the fact that a particular DFD may be a special case of other DFD's and thus may have already been counted, although incorrectly. Evaluation of the coefficient requires compensating for this previous incorrect inclusion. This may be done without knowledge of the interactions or lattice type. The lattice sum simply involves doing sums over the lattice vectors with the summand being products of the $J_{\vec{r}_i}$ and the appropriate δ -function restrictions. Evidently, the lattice sum requires knowledge about the interactions and the lattice type.

Consider the evaluation of the coefficient $C_n(\text{DFD})$ of a particular DFD occurring in R_n . The first step is to construct the graph it describes. The coefficient is calculated according to the following rules⁶:

(a) The selection of a direction for each vector requires a factor of $2^{n-s}/2^n = 2^{-s}$, where s is the number of disjoint components in the original graph. (The convention used here is that $s=1$ for a connected graph.) At this point if $s > 1$, i. e., the original graph is not connected, then one must construct the possibly several different ways of connecting the various components. For each construction, steps (b)–(d) listed below must be performed. The reason the graph must be connected is because only connected graphs make a contribution of order N in Z^N .

(b) A repetition factor $(1/n!)(n!/g)$ enters, where g is the number of symmetry operations that transforms a graph into itself.

(c) There is a permutation factor p , where p is the number of ways in which the graph may be constructed once two points in the graph have been connected.

(d) To each vertex joined by b (b even) bonds, we associate a semi-invariant factor M_b^0 . The coefficient of the DFD is then given by

$$C_n(\text{DFD}) = (a) \times \sum [(b) \times (c) \times (d)] \quad (6)$$

where (i) represents the number resulting from step (i) above and the sum is performed over the various ways of connecting the disjoint components of the original graph.

The first factor in rule (a) results from selecting a direction (two possibilities for each vector) for the remaining vectors in a connected component relative to one given vector. The factor of 2^n in the denominator results from removal of the $\frac{1}{2}^n$ occurring in the inner summand of Eq. (4).

The factor of $1/n!$ in rule (b) accounts for the removal of $1/n!$ in Eq. (4). The factor of $n!/g$ takes into account the labeling of the vectors in the graph to form the DFD with g occurring to compensate for the identical labeling of certain vectors or groups of vectors.

In rule (c), the p factor results from the number

of different ways of constructing (ordering of the vectors) the graphs having the same DFD.

The factor M_b^0 in rule (d) compensates for the incorrect contribution introduced by other DFD's of which this particular DFD is a special case. The value of M_b^0 is the coefficient of $x^{b-1}/(b-1)!$ in the expansion of $\tanh x$ as has been determined previously by several authors.³ This result is derived in the Appendix by using an approach based on the "overcounting" mentioned earlier.

The lattice sum $L_n(\text{DFD})$ of a particular DFD occurring in R_n is given by

$$L_n(\text{DFD}) = \sum_{\vec{r}_1} \sum_{\vec{r}_2} \cdots \sum_{\vec{r}_n} \left[\left(\prod_{i=1}^n J_{\vec{r}_i} \right) \delta(\text{DFD}) \right], \quad (7)$$

where $\delta(\text{DFD})$ is the product of δ functions that are the DFD.

In summary, for a given value of n in Eq. (5), the different DFD's are listed, a step that is most conveniently done by drawing the different graphs and applying the DFD. The values of $C_n(\text{DFD})$ and $L_n(\text{DFD})$, defined in Eqs. (6) and (7), are calculated for each DFD. The term R_n is then given by

$$R_n = \sum_{\text{DFD}} C_n(\text{DFD}) L_n(\text{DFD}), \quad (8)$$

where \sum_{DFD} is a sum over the different DFD's.

III. RESULTS FOR fcc LATTICE AND $J_1, J_2, J_3, \neq 0$

The high-temperature expansion of $\ln Z$ is expected to have the asymptotic form²

$$\ln Z \sim \frac{D(\beta/\beta_c)^n}{(n+a)^{5/8}}. \quad (9)$$

Several of the quantities that are calculable directly from $\ln Z$ are expected to have the following asymptotic form in their high-temperature expansion:

$$\begin{aligned} E, \quad \alpha_i &\sim \frac{D(\beta/\beta_c)^n}{(n+a)^{15/8}}, \quad i=1, 2, 3 \\ C, \quad \frac{\partial \alpha_i}{\partial T} &\sim \frac{D(\beta/\beta_c)^n}{(n+a)^{7/8}}, \quad i=1, 2, 3 \end{aligned} \quad (10)$$

where $\alpha_i = \langle \sigma_i \sigma_{i+j} \rangle$ is the correlation coefficient connecting i th neighbors, $E = -\frac{1}{2} \sum_i J_i \alpha_i$ is the energy per site, and C is the specific heat. Of course, the quantities D and a differ for each of the functions.

Here, the R_n is identical to the previously defined R_n only for $\ln Z$. For the other functions, a redefinition follows from the operation on $\ln Z$ that is required to produce that particular function, e. g.,

$$\begin{aligned} \alpha_i &= \frac{2}{z_i} \frac{\partial \ln Z}{\partial \beta J_i}, \quad i=1, 2, 3 \\ C &= k \beta^2 \frac{\partial^2 \ln Z}{\partial \beta^2}, \end{aligned} \quad (11)$$

where z_i is the number of i th neighbors.

The model considered is that of a fcc lattice having first-, second-, and third-neighbor interactions (J_1, J_2, J_3). Terms through $n=9$ of R_n were calculated and expressed in terms of J_1, J_2 , and J_3 . The expansion is given in Table I. Values of T_c and values of α_1, α_2 , and α_3 at $T=T_c$ were calculated for ratios of J_2/J_1 and J_3/J_1 each varying between 0 and 2. Although only ferromagnetic couplings ($J_i > 0$) have been considered, the identical calculations could be performed for antiferromagnetic couplings ($J_i < 0$) or mixed ferromagnetic and antiferromagnetic couplings. The calculation of T_c was done by means of the ratio method in which it has been assumed that the early terms of the series have assumed the form given by Eq. (10) for the various functions. (This assumption is implied by any type of calculation that uses a finite number of terms from an infinite series.)

The assumption is that one may write

$$R_n \beta^n = \frac{D(\beta/\beta_c)^n}{(n+a)^b} \quad (12)$$

or

$$\frac{R_n}{[J(\vec{k}_m)]^n} = \frac{D}{(n+a)^b [\beta_c J(\vec{k}_m)]^n}, \quad (13)$$

where b has the appropriate value given in Eq. (10) and

$$J(\vec{k}_m) = 12J_1 + 6J_2 + 24J_3 \quad (14)$$

is the maximum value of the Fourier transform of the $\{J_i\}$ for ferromagnetic coupling. To eliminate the parameter D , one may write

$$RD_n = J(\vec{k}_m) R_n / R_{n+1} = \beta_c J(\vec{k}_m) [(n+a+1)/(n+a)]^b. \quad (15)$$

One approach⁷ is to expand

$$[(n+a+1)/(n+a)]^b \simeq 1 + b/(n+a). \quad (16)$$

The values $RD_n, n=1, 2, \dots, 8$ are calculated and plotted versus $1/(n+a)$. The value of a is selected such that the plotted values most nearly lie on a straight line whose ratio of slope to intercept is b . This is a difficult task and does not appear to be well suited for the limited number of terms given. Likewise, the method of Padé approximants⁷ is inconclusive.

There is a method that is more straightforward in which values of three consecutive R_n (or two consecutive RD_n) are used. In this method, $\beta_c J(\vec{k}_m)$ is eliminated by writing

$$RDD_n = RD_n / RD_{n+1} = (n+a+1)^{2b} / [(n+a)(n+a+2)]^b. \quad (17)$$

Values of a are determined from the above equation for $n=5, 6, 7$. Values of $\beta_c J(\vec{k}_m)$ are then calculated for $n=8$ by use of Eq. (15). Of course, the values of a obtained from Eq. (17) for the various values of n differ, and the corresponding

values of $\beta_c J(\vec{k}_m)$ resulting from Eq. (15) for $n=8$ differ. The accuracy in a final determined value of $\beta_c J(\vec{k}_m)$ could be measured by the closeness of the values of $\beta_c J(\vec{k}_m)$ calculated by the method outlined above.

Calculations of $\beta_c J(\vec{k}_m)$ have been performed using the expansions of $\ln Z, \alpha_1$, and $\partial \alpha_i / \partial T, i=1, 2, 3$, and C . We have found that the values of $\beta_c J(\vec{k}_m)$ differ less for the expansion of α_1 than for any of the other functions. It is expected that near-neighbor correlation coefficients should assume their asymptotic form more quickly than do far-neighbor correlation coefficients. However, it may be surprising that α_1 is singled out since it does not diverge at $T=T_c$ while C and $\partial \alpha_i / \partial T, i=1, 2, 3$, do diverge. Nevertheless, our conclusion is that α_1 is the most reliable of the functions calculated, and the values of T_c have been determined using the high-temperature expansion of this function. The results are given in Table II.

For most values of J_2/J_1 and J_3/J_1 , the three calculated values of $\beta_c J(\vec{k}_m)$ were within 0.2% of each other. There are exceptions in which the agreement is not as good—most notably for J_2/J_1 and/or $J_3/J_1=0$. This might be expected since for $J_2/J_1=0$ interactions between closer neighbors (second) have been neglected while interactions between the more distant neighbors (third) have been included. For $J_3/J_1=0$ and as J_2/J_1 increases in value, one has to contend with second neighbors

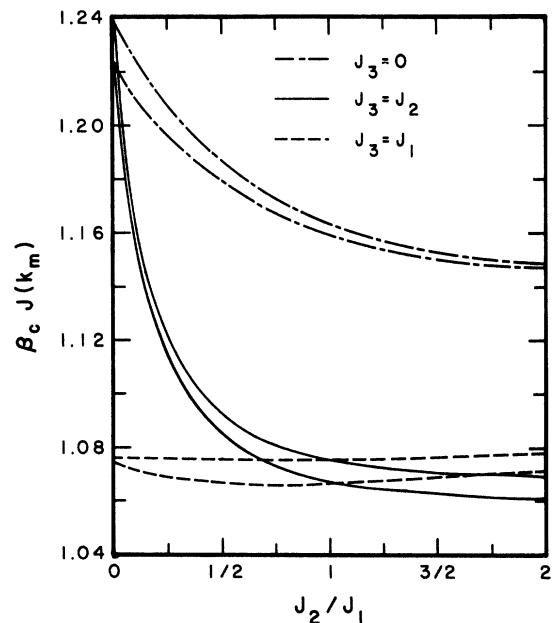


FIG. 1. Graph of $\beta_c J(\vec{k}_m)$ vs J_2/J_1 for several representative values of J_3/J_1 . For each value of J_3/J_1 , the upper curve is that of the generalized spherical model (Ref. 5) and the lower curve is that of the Ising model.

TABLE I. (Continued)

	q/p	0	1	2	3	
	0	35 198.06 (4 038 300)	167 948.8 (13 305 600)	332 311.6 (20 049 120)	348 848 (17 015 040)	
	1	689 726.4 (44 150 400)	2 754 141 (135 072 000)	4 424 995 (179 424 000)	3 622 464 (131 927 040)	
	2	5 402 966 (236 540 640)	17 722 968 (631 370 880)	22 556 268 (715 982 400)	13 982 528 (425 510 400)	
	3	22 291 354 (752 451 840)	58 592 784 (1 709 164 800)	57 225 392 (1 567 641 600)	25 499 840 (708 019 200)	
$n=8$	4	53 807 597 (1 557 365 040)	109 071 360 (2 849 172 480)	76 968 672 (1 991 727 360)	22 172 128 (598 671 360)	
	5	78 648 877 (2 096 666 880)	115 624 790 (2 912 555 520)	52 607 827 (1 368 783 360)	7 389 152 (202 460 160)	
	6	68 571 740 (1 812 404 160)	65 135 472 (1 679 166 720)	14 405 128 (407 111 040)		
	7	32 832 909 (898 813 440)	15 126 746 (412 715 520)			
	8	6 656 199 (203 858 760)				
	q/p	4	5	6	7	8
	0	206 104 (9 918 720)	65 625.6 (2 983 680)	11 125.6 (1 028 160)	0 (0)	147.0798 (44 730)
	1	1 593 760 (61 770 240)	352 262.4 (14 676 480)	44 262.4 (3 225 600)	0 (0)	
$n=8$	2	4 448 424 (153 296 640)	626 448 (23 869 440)	40 134 (2 913 120)		
	3	5 236 448 (172 892 160)	368 851.2 (12 902 400)			
	4	2 202 635 (76 623 120)				
	q/p	0	1	2	3	
	0	242 065.6 (40 958 400)	1 303 961 (156 038 400)	3 003 053 (269 136 000)	3 803 612 (277 804 800)	
	1	5 431 762 (527 325 120)	25 176 021 (1 859 820 480)	48 525 626 (2 896 871 040)	50 101 671 (2 614 792 320)	
	2	50 555 463 (3 279 443 328)	197 733 683 (10 336 588 416)	313 155 715 (14 023 933 056)	256 320 736 (10 721 531 520)	
	3	254 998 277 (12 390 928 704)	829 156 162 (33 936 791 616)	1 052 468 376 (38 890 152 000)	663 832 583 (24 034 429 440)	
	4	783 446 673 (30 973 525 632)	2046 014 528 (71 535 744 000)	2 005 933 328 (66 098 592 000)	914 954 848 (30 979 670 400)	
$n=9$	5	1 514 536 508 (52 754 889 600)	3 091 146 524 (98 186 739 840)	2 185 408 876 (68 565 450 240)	646 123 599 (21 614 826 240)	
	6	1 862 086 458 (60 861 669 120)	2 746 035 232 (85 691 571 840)	1 268 051 590 (40 015 019 520)	234 863 551 (6 431 846 400)	
	7	1 412 656 071 (45 750 519 360)	1 351 065 280 (43 159 919 040)	303 854 400 (10 029 821 760)		
	8	602 381 304 (20 290 314 240)	281 161 541 (9 724 942 080)			
	9	110 764 114 (3 990 604 800)				

(being vectors of a sc lattice) making a greater contribution to the n even terms than the n odd terms.

For comparison, the value of $\beta_c J(\vec{k}_m)$ obtained by Domb and Dalton⁸ in an analysis of the high-temperature expansion of the susceptibility for $J_1=J_2$ and $J_3=0$ is 1.1601 compared to our value of 1.160, and for $J_1=J_2=J_3$ it is 1.079 compared to our value

of 1.067; the value obtained by Fisher and Sykes⁹ for $J_2=J_3=0$ is 1.2252 compared to our value of 1.223.

The values of $\beta_c J(\vec{k}_m)$ have been plotted in Fig. 1 for several representative cases of the interactions. The curve of $J_3/J_1=1$ and J_2/J_1 increasing shows $\beta_c J(\vec{k}_m)$ increasing for larger values of

TABLE I. (Continued)

q/p	4	5	6	7	8	9
0	2 867 616 (181 440 000)	1 297 244 (85 881 600)	331 507.2 (22 014 720)	48 665.75 (6 441 120)	0 (0)	0 (0)
1	29 635 128 (1 459 745 280)	10 125 596 (555 932 160)	1 819 098 (110 496 960)	188 262.7 (21 591 360)	0 (0)	
2	115 825 824 (4 837 916 160)	28 667 712 (1 404 527 040)	3 301 382 (184 705 920)	177 837.1 (18 869 760)		
3	216 036 736 (8 202 357 880)	34 669 458 (1 614 513 600)	1 987 360 (102 392 640)			
4	193 415 104 (7 052 451 840)	15 079 556 (717 050 880)				
5	66 681 504 (2 434 199 040)					

J_2/J_1 . The value of $\beta_c J(\vec{k}_m)$ ultimately would have to increase for this case since as $J_2/J_1 \rightarrow \infty$ the structure becomes that of a sc lattice with first-neighbor interactions.

The ratio $T_c(J_2/J_1)/T_c(0)$ varies almost linearly with J_2/J_1 , where $T_c(x)$ is the transition temperature for a given value of x . This fact has been observed by Dalton and Wood¹⁰ for the special case of $J_3=0$ with $0 \leq J_2/J_1 \leq 1$. We have taken the values of $\beta_c J(\vec{k}_m)$ determined in this paper and have calculated the ratios for the special case of $J_3=0$. The ratios agree with those of Dalton and Wood to within a fraction of a percent.

The curve in Fig. 2 can be approximated by

$$\frac{T_c(J_2/J_1)}{T_c(0)} = 1 + m J_2/J_1 \quad (18)$$

Actually the curve is convex so that the effective value of m decreases as J_2/J_1 increases. For example, in the range $0 \leq J_2/J_1 \leq \frac{1}{2}$, $m \approx 0.62$ and in the range $\frac{1}{2} \leq J_2/J_1 \leq 2$, $m \approx 0.55$. The variation in m seems to be sufficiently small so that the linear approximation of Eq. (18) is helpful.

We have also calculated ratios for $0 \leq J_2/J_1 = J_3/J_1 \leq 2$, i. e., J_2 and J_3 increasing at the same rate. We find with an adjustment of the scale of $T_c(J_2/J_1)/T_c(0) - 1$ that the curve for this case lies almost exactly on the curve drawn in Fig. 2 for $J_3=0$ and $0 \leq J_2/J_1 \leq 2$. The value of m in Eq. (18) for $J_2=J_3$ is approximately a factor of 5.17 times the value of m for $J_3=0$. The curve for $J_3=1$ and $0 \leq J_2/J_1 \leq 2$ has similar properties with the appropriate value of m being a factor of 0.30 times the value of m for $J_3=0$. Likewise, the curve for $J_2=1$ and $0 \leq J_3/J_1 \leq 2$ (J_3/J_1 plotted along the horizontal axis) is similar to the curve in Fig. 2 with the appropriate value of m being a factor of 2.55 times the value of m for $J_3=0$.

The values of $\beta_c J(\vec{k}_m)$ were then used to calculate the values of α_1 , α_2 , and α_3 at $T = T_c$. The terms known for these functions were included in their exact form and then the value of the remain-

ing terms in their infinite series was calculated by using their asymptotic form. The values are given in Table II. The uncertainty in the calculated values of the correlation coefficients is estimated to be 1%. The uncertainty in $\beta_c J(\vec{k}_m)$ is compounded in calculating the correlation coefficients since powers of $\beta_c J(\vec{k}_m)$ are involved. Also, an additional parameter D in Eq. (10) must be determined.

The values of the correlation coefficients have been plotted in Figs. 3-5 for the same cases of interactions as in Fig. 1 for $\beta_c J(\vec{k}_m)$. A particular

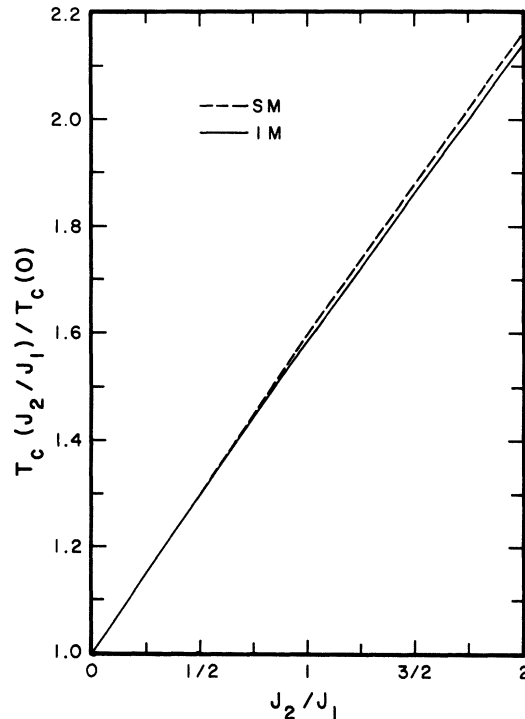


FIG. 2. Graph of the transition temperature versus increasing second-neighbor interaction for the special case of $J_3=0$, where SM denotes the spherical model, and IM the Ising model.

correlation coefficient depends on the relationship among the three interactions. Correlations between given neighbors may result not only from interactions between those neighbors but also from interactions between other neighbors. This is the reason for the varying behavior of the α_i .

IV. COMPARISON OF RESULTS OF THE ISING MODEL AND GENERALIZED SPHERICAL MODEL

The spherical model⁴ is obtained by replacing the conditions $\sigma_j = \pm 1$, ($j = 1, 2, \dots, N$) by the one condition

$$\frac{1}{N} \sum_{j=1}^N \sigma_j^2 = 1 .$$

The transition temperature is obtained by evaluating

$$2S_c = \frac{1}{\gamma} \int_{\gamma} d^3k \left(1 - \frac{J(\vec{k})}{J(\vec{k}_m)} \right)^{-1} , \quad (19)$$

where $J(\vec{k})$ is the Fourier transform of the interactions, $J(\vec{k}_m)$ is the maximum value of $J(\vec{k})$, and the integration is over a unit cell γ in the reciprocal

space.

The integral is evaluated by expanding the function $[1 - J(\vec{k})/J(\vec{k}_m)]^{-1}$ and performing the integrals of $(1/\gamma) \int_{\gamma} [J(\vec{k})]^n d^3k$ for limited values of n . The asymptotic form of this integral is determined to complete the approximate evaluation of the series.¹¹

This integral may also be written as

$$\frac{1}{\gamma} \int_{\gamma} [J(\vec{k})]^n d^3k = \sum_{\vec{r}_1} \sum_{\vec{r}_2} \dots \sum_{\vec{r}_n} \left(\prod_{i=1}^n J_{\vec{r}_i} \right) \delta_{\vec{r}_1 + \vec{r}_2 + \dots + \vec{r}_n, 0} . \quad (20)$$

Thus the integral is the lattice sum, defined in Eq. (7) for the DFD $\delta_{\vec{r}_1 + \vec{r}_2 + \dots + \vec{r}_n, 0}$. This is a basic lattice sum which is used to calculate the lattice sums of other DFD's. The evaluation of the integral in Eq. (20) for $n = 2, 3, \dots, 9$ is expressed in terms of J_1 , J_2 , and J_3 in Table I.

In the usual spherical model, the identification is

$$2S_c = \beta_c J(\vec{k}_m) . \quad (21)$$

A generalized spherical model⁵ has been defined in which the transition temperature is given by

TABLE II. Values of $\beta_c J(\vec{k}_m)$, α_1 , α_2 , and α_3 at $T = T_c$ (listed in that order) for various ratios of J_2/J_1 and J_3/J_1 .

J_3/J_1 \ J_2/J_1	0	$\frac{1}{8}$	$\frac{1}{4}$	$\frac{1}{2}$	$\frac{3}{4}$	1	$\frac{3}{2}$	2
0	1.223	1.207	1.196	1.180	1.167	1.160	1.151	1.147
	0.2457	0.2350	0.2269	0.2125	0.1985	0.1880	0.1697	0.1554
	0.1610	0.1609	0.1623	0.1647	0.1652	0.1674	0.1707	0.1737
	0.1374	0.1324	0.1293	0.1234	0.1163	0.1116	0.1027	0.0953
$\frac{1}{8}$	1.156	1.148	1.142	1.135	1.129	1.127	1.125	1.124
	0.1917	0.1860	0.1810	0.1734	0.1655	0.1598	0.1492	0.1394
	0.1242	0.1264	0.1289	0.1346	0.1385	0.1434	0.1509	0.1562
	0.1136	0.1108	0.1086	0.1058	0.1021	0.1000	0.0955	0.0905
$\frac{1}{4}$	1.124	1.119	1.114	1.110	1.108	1.107	1.108	1.109
	0.1606	0.1571	0.1533	0.1486	0.1445	0.1407	0.1342	0.1277
	0.1046	0.1075	0.1098	0.1161	0.1220	0.1271	0.1363	0.1431
	0.1019	0.1002	0.0980	0.0963	0.0948	0.0932	0.0908	0.0875
$\frac{1}{2}$	1.095	1.091	1.087	1.085	1.085	1.085	1.087	1.090
	0.1263	0.1241	0.1217	0.1196	0.1182	0.1164	0.1135	0.1108
	0.0848	0.0872	0.0892	0.0954	0.1015	0.1067	0.1162	0.1243
	0.0912	0.0897	0.0879	0.0871	0.0867	0.0860	0.0849	0.0830
$\frac{3}{4}$	1.081	1.078	1.075	1.073	1.073	1.074	1.076	1.079
	0.1069	0.1056	0.1042	0.1029	0.1022	0.1018	0.1005	0.0993
	0.0743	0.0765	0.0765	0.0839	0.0894	0.0947	0.1038	0.1118
	0.0857	0.0847	0.0835	0.0827	0.0825	0.0825	0.0821	0.0817
1	1.074	1.072	1.069	1.067	1.066	1.067	1.069	1.072
	0.0949	0.0943	0.0931	0.0922	0.0916	0.0916	0.0912	0.0910
	0.0682	0.0705	0.0722	0.0769	0.0815	0.0864	0.0951	0.1028
	0.0830	0.0823	0.0812	0.0804	0.0799	0.0801	0.0802	0.0804
$\frac{3}{2}$	1.067	1.066	1.064	1.062	1.062	1.062	1.063	1.064
	0.0805	0.0804	0.0799	0.0794	0.0796	0.0797	0.0799	0.0798
	0.0613	0.0634	0.0650	0.0688	0.0730	0.0770	0.0845	0.0909
	0.0801	0.0798	0.0791	0.0785	0.0785	0.0785	0.0787	0.0786
2	1.065	1.064	1.062	1.060	1.060	1.060	1.060	1.061
	0.0727	0.0726	0.0721	0.0718	0.0722	0.0724	0.0726	0.0730
	0.0580	0.0597	0.0609	0.0640	0.0677	0.713	0.0777	0.0838
	0.0791	0.0788	0.0782	0.0776	0.0776	0.0777	0.0777	0.0780

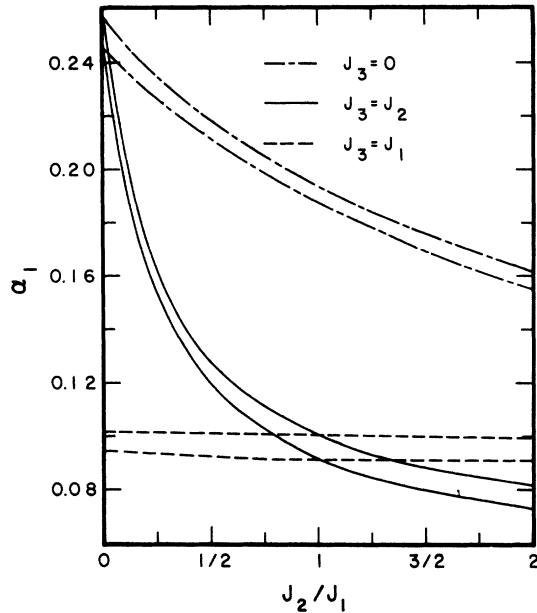


FIG. 3. Graph of α_1 vs J_2/J_1 for several representative values of J_3/J_1 . For each value of J_3/J_1 , the upper curve is that of the generalized spherical model (Ref. 5) and the lower curve is that of the Ising model.

$$\sinh \beta_c J(\vec{k}_m) = 2S_c \sinh 1. \quad (22)$$

The values of $\beta_c J(\vec{k}_m)$, α_1 , α_2 , and α_3 are plotted in Figs. 1, 3, 4, and 5, respectively, for several cases of interactions.

An interesting observation from Fig. 1 is that the generalized spherical model has a higher value of $\beta_c J(\vec{k}_m)$ than does the Ising model. The general properties of $\beta_c J(\vec{k}_m)$ as a function of the ratios J_2/J_1 and J_3/J_1 are similar for the generalized spherical model and Ising model. For the case of $J_3/J_1 = 1$ and J_2/J_1 varying, both have the minimum value of $\beta_c J(\vec{k}_m)$ occurring at the value of $J_2/J_1 \approx \frac{3}{4}$.

Observance of Fig. 2 shows that the ratio $T_c(J_2/J_1)/T_c(0)$ of the spherical model is very close to that of the Ising model. The curves of the spherical model for other cases (those mentioned in Sec. III) are likewise very close to those of the Ising model.

It is seen from Figs. 3-5 that the correlation coefficients of the generalized spherical model and Ising model have similar behavior as functions of the ratios J_2/J_1 and J_3/J_1 .

ACKNOWLEDGMENT

I wish to thank G. L. Hall for his valuable suggestions and criticisms.

APPENDIX

The semi-invariant factor M_b^0 enters because of the correction that has to be made for overcounting,

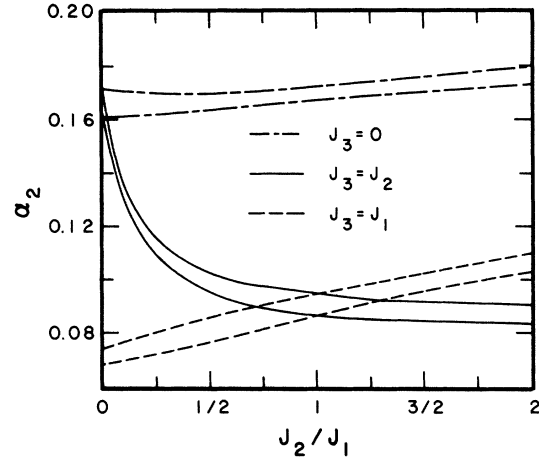


FIG. 4. Graph of α_2 vs J_2/J_1 for several representative values of J_3/J_1 . For each value of J_3/J_1 , the upper curve is that of the generalized spherical model (Ref. 5) and the lower curve is that of the Ising model.

i.e., inclusion of specialized DFD's in more general DFD's. The derivation that follows has as its basis an inspection of the degree (the number of bonds) of a vertex and the subtraction of the incorrect contributions made by those terms whose vertices if coalesced have collectively the degree of this one vertex.

Consider a vertex of degree $2n$. If the incorrect contributions are compensated for, the vertex will have a resultant weight of unity. The procedure is to enumerate the different ways in which this one vertex of degree $2n$ may be formed by joining together several vertices, each having an even de-

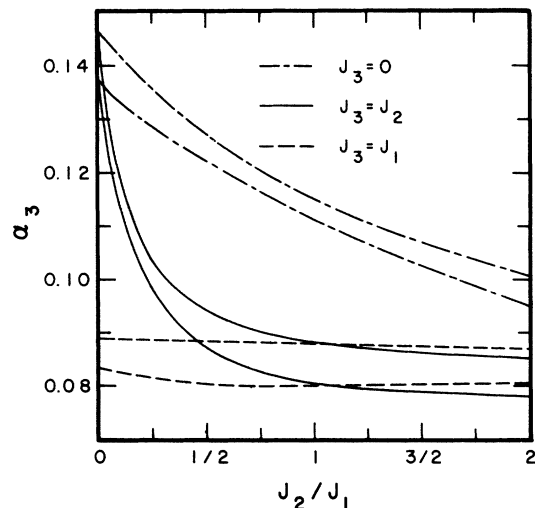


FIG. 5. Graph of α_3 vs J_2/J_1 for several representative values of J_3/J_1 . For each value of J_3/J_1 , the upper curve is that of the generalized spherical model (Ref. 5) and the lower curve is that of the Ising model.

gree. We associate the characteristic semi-invariant factors with each combination of vertices. If one combines the semi-invariant factors with the number of ways that the single vertex may be resolved into the several vertices, and then performs a sum over the various decompositions, one will get the correct weight of unity. The equation reads

$$1 = \sum_{j=1}^n \left[\sum'_{m_1, m_2, \dots, m_j} \binom{2n}{2m_1, 2m_2, \dots, 2m_j} \left(\prod_{i=1}^j M_{2m_i}^0 \right) \right], \quad (\text{A1})$$

where j is the number of different vertices in the decomposition and the prime on the second sum means $\sum_{i=1}^j 2m_i = 2n$ for the $2m_i$ having possible

values from 2 to $2n$.

The set of equations for $n=1, 2, \dots$ will generate the values of M_2^0, M_4^0, \dots . But the semi-invariant M_{2n}^0 is also the coefficient of $x^{2n-1}/(2n-1)!$ in the expansion of $\tanh x$. This identification follows from writing the expansion of $\tanh x$, integrating to produce $\ln(\cosh x)$, and then taking the exponential to produce $\cosh x$. The final step is to equate the coefficient of x^{2n} in the expansion of $\cosh x$ and in the expression resulting from the operations described in the above statement. It will be seen that the recursion relation obtained for the coefficient in the expansion of $\tanh x$ is identical to the recursion relation in Eq. (A1) of the semi-invariants.

¹For a general review of the Ising model and the method of the high-temperature expansion, see C. Domb, *Advan. Phys.* **9**, 149 (1960); **9**, 245 (1960).

²M. F. Sykes, J. L. Martin, and D. L. Hunter, *Proc. Phys. Soc. (London)* **91**, 671 (1967).

³For example, see G. Horowitz and H. Callen, *Phys. Rev.* **124**, 1757 (1961); M. Coopersmith and R. Brout, *ibid.* **130**, 2539 (1963); F. Englert, *ibid.* **129**, 567 (1963); R. Brout, *Phase Transitions* (Benjamin, Amsterdam, 1965), pp. 33-38.

⁴The spherical model is defined by T. H. Berlin and M. Kac, *Phys. Rev.* **86**, 821 (1952).

⁵The "generalized" spherical model is defined by J. Philhours and G. L. Hall, *Phys. Rev.* **177**, 976 (1969).

⁶Rules (b) and (d) are given in R. Brout, *Phase Transitions* (Benjamin, Amsterdam, 1965), p. 36, as his rules (4) and (3), respectively.

⁷G. A. Baker, Jr., in *Advances in Theoretical Physics*, edited by K. A. Brueckner (Academic, New York, 1965), Vol. I.

⁸C. Domb and N. W. Dalton, *Proc. Phys. Soc. (London)* **89**, 859 (1966).

⁹M. E. Fisher and M. F. Sykes, *Physica* **28**, 959 (1962).

¹⁰N. W. Dalton and D. W. Wood, *J. Math. Phys.* **10**, 1271 (1969).

¹¹M. Lax, *Phys. Rev.* **97**, 629 (1954).

Magnetic Excitations in Antiferromagnetic CoF_2 . I. Spin-Optical-Phonon Interaction

S. J. Allen, Jr. and H. J. Guggenheim

Bell Telephone Laboratories, Murray Hill, New Jersey 07974

(Received 11 January 1971)

The interaction of the low-lying magnons and excitons with the E_g optical phonon in antiferromagnetic CoF_2 is directly observed by measuring the magnetic-dipole intensity transferred from magnetic excitations to the otherwise optically inactive E_g lattice mode. The anomalous behavior of the frequency, linewidth, and magnetic-dipole intensity of this phonon have been measured as the temperature is raised from 4.2°K through the Néel point (37.7°K) to $\sim 4.5T_N$ (180°K). The frequency drops continuously with a break in slope at the Néel point, while the linewidth narrows by more than a factor of 3 when the temperature passes through the Néel point. A theory of the temperature dependence of the transferred intensity is derived which distinguishes two contributions. The first is proportional to the sublattice magnetization and vanishes in the paramagnetic state; the second is proportional to the square of the Boltzmann factor for the exciton states and vanishes only at arbitrarily high temperature. By fitting the experimental temperature dependence of the intensity to the theory, the local spin-lattice-interaction parameters for the E_g distortions can be determined.

I. INTRODUCTION

Unquenched orbital motion in the single-ion ground state of Co^{2+} significantly alters the mag-

netic properties of the two-sublattice antiferromagnet CoF_2 . The magnetic structure¹ consists of moments parallel and antiparallel to the tetragonal axis of the rutile crystal structure and is the